Journal of Biomolecular NMR, **17:** 265–268, 2000.
KLUWER/ESCOM

Measurement of the protein backbone dihedral angle φ based on quantification of remote CSA/DD interference in inter-residue $^{13}C'(i-1)$-$^{13}C^{\alpha}(i)$ multiple-quantum coherences

Karin Kloiber & Robert Konrat*
Institute of Organic Chemistry, University of Innsbruck, Innrain 52a, A-6020 Innsbruck, Austria

Received 22 February 2000; Accepted 9 May 2000

Key words: chemical shift anisotropy, cross-correlated spin relaxation, dihedral angles, multiple-quantum coherence, structure determination

Abstract

A novel triple-resonance NMR method is presented for the measurement of the protein backbone dihedral angle φ based on differential multiple-quantum relaxation induced by relaxation interference between $^{1}H^{\alpha}(i)$-$^{13}C^{\alpha}(i)$ dipolar and $^{13}C'(i-1)$ (carbonyl) chemical shift anisotropy mechanisms. The method employs a simultaneous transfer of ^{15}N magnetization to the inter- and intra-residue $^{13}C^{\alpha}$ carbons as well as the directly attached carbonyl carbon $^{13}C'$. Results obtained on ^{13}C,^{15}N-labeled ubiquitin demonstrate the potential of the method.

Recently, NMR methods for the measurement of cross-correlation spin relaxation rates have been devised that complement or even substitute more conventional approaches like NOEs or scalar coupling constants to local structure determination of proteins by NMR. The methods rely on quantification of cross-correlated fluctuations of different dipolar couplings (Reif et al., 1997; Chiarparin et al., 1999; Pelupessy et al., 1999) or dipolar couplings and anisotropic chemical shifts, respectively (Yang and Kay, 1998; Yang et al., 1997, 1998). The particularly attractive feature of these experiments is the fact that no empirical calibration (Karplus relation) is needed.

However, a limitation of angle determination by the use of cross-correlated spin relaxation is the multiplicity of dihedral angles related to only a single relaxation rate. It has been shown for the dihedral angle Ψ (Yang and Kay, 1998) that the number of possible dihedral angles can be considerably reduced by combining measurements from $^{13}C^{\alpha}$-$^{1}H^{\alpha}$ dipolar ^{15}N-$^{1}H^{N}$ dipolar or $^{13}C^{\alpha}$-$^{1}H^{\alpha}$ dipolar $^{13}C'$ CSA cross-correlation rates, leading to unambiguous determination of dihedral angles in favorable cases. A similar solution is still wanting for the determination of the protein backbone dihedral angle φ, for which an experiment has been devised based on the quantification of $^{13}C^{\alpha}$-$^{1}H^{\alpha}$ dipolar/^{15}N-$^{1}H^{N}$ dipolar cross-correlation rates (Pelupessy et al., 1999). With this in mind, we present a triple resonance pulse scheme for measuring $^{13}C^{\alpha}(i)$-$^{1}H^{\alpha}(i)$/$^{13}C'(i-1)$ dipolar/CSA cross-correlation rates which are related to φ. The method relies on a simultaneous magnetization transfer from $^{15}N(i)$ to both the intraresidue $^{13}C^{\alpha}(i)$ and the preceding $^{13}C^{\alpha}(i-1)$, as well as the directly attached carbonyl carbon $^{13}C'(i-1)$. The resulting longitudinal three-spin orders $4N_z(i)C^{\alpha}_z(i)C'_z(i-1)$ and $4N_z(i)C^{\alpha}_z(i-1)C'_z(i-1)$ are subsequently converted into two-spin coherences involving either $C^{\alpha}_{x,y}(i)C'_{x,y}(i-1)$ or $C^{\alpha}_{x,y}(i-1)C'_{x,y}(i-1)$, which evolve during a constant time period T_C comprising the indirect evolution period t_1. The pulse sequence is shown in Figure 1.

As in the experiment by Yang et al. (1998), we applied simultaneous 180° pulses to the $^{13}C^{\alpha}$ and $^{1}H^{\alpha}$ nuclei in the middle of the constant time delay T_C, in order to average the multiple-quantum relaxation rates related by spin inversion of $^{13}C^{\alpha}$ and $^{1}H^{\alpha}$. In contrast to the one-bond scalar coupling be-

*To whom correspondence should be addressed. E-mail: robert.konrat@uibk.ac.at

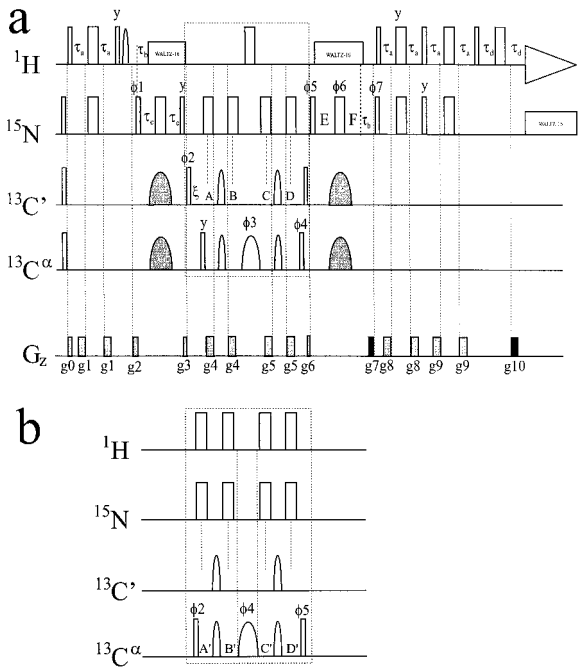

Figure 1. (a) Pulse scheme for the measurement of $^{13}C'$-$^{13}C^\alpha$ multiple-quantum relaxation. Narrow and wide pulses indicate 90° and 180° pulses, respectively, and, unless indicated, all pulses are applied along the x-axis. ^{15}N pulses use a 6 kHz field, with WALTZ (Shaka et al., 1983) decoupling achieved with a 1 kHz field. Simultaneous inversion of both $^{13}C'$ and $^{13}C^\alpha$ is achieved using an adiabatic WURST inversion pulse (Kupce and Freeman, 1995) (500 μs, 80 kHz sweep width, center of sweep at 175 ppm, 3.3 kHz peak radiofrequency (rf), 30% truncation level). The $^{13}C'$ shaped pulses have r-SNOB profiles (Kupce et al., 1995) (390 μs) while the $^{13}C^\alpha$ shaped pulses make use of RE-BURP profiles (Geen and Freeman, 1991). The non-selective $^{13}C^\alpha$ refocusing pulses are 400 μs while the selective $^{13}C^\alpha$ refocusing pulse with phase ϕ3 is 2 ms (excitation centered at 55 ppm). Note that the $^{13}C'$ and $^{13}C^\alpha$ refocusing pulses are not applied simultaneously, but the higher power $^{13}C^\alpha$ pulses are applied prior to the $^{13}C'$ pulses in both cases, compensating the Bloch–Siegert effects on the $^{13}C'$ magnetization (Vuister and Bax, 1992; Yang et al., 1998). The delay ξ is inserted to compensate for $^{13}C'$ shift evolution during the selective RE-BURP (pw_{REBURP}) and the 90° $^{13}C^\alpha$ pulses flanking the constant-time period (A+B+C+D), ($\xi = pw_{REBURP} - 2 * pw_{90}(^{13}C^\alpha)$). The values for τ_a, τ_b, τ_c and τ_d were set to 2.25, 5.3, 12.4 and 0.75 ms, respectively. $A = (T_C + t_1)/4$; $B = (T_C - t_1)/4$; $C = (T_C - t_1)/4$; $D = (T_C + t_1)/4$; $E = (T_N - t_2)/2$; $F = (T_N + t_2)/2 - \tau_b$; $T_C = 26$ ms; $T_N = 24.8$ ms. The phase cycling was $\phi1 = x, -x$; $\phi2 = -x, x, x, -x$; $\phi3 = 8(x), 8(y), 8(-x), 8(-y)$; $\phi4 = 4(y), 4(-y)$, $\phi5 = y$, $\phi6 = 4(x), 4(-x)$, $\phi7 = x$; and receiver 2(x),4(−x),2(x),2(−x),4(x),2(−x). Quadrature detection in F_1 is achieved by States-TPPI of ϕ2 (Marion et al., 1989) while quadrature detection in F_2 employs the enhanced sensitivity pulsed field gradient method (Kay et al., 1992; Schleucher et al., 1993) where for each value of t_2 separate data sets are recorded for (g7, ϕ7) and (−g7, ϕ7 + 180°). For each successive t_2 value, ϕ5 and the phase of the receiver are incremented by 180°. (b) Scheme to record the 'reference' experiment. The pulses in the boxed region are replaced by the scheme indicated in b. $A' = (T_C + t_1)/4$; $B' = (T_C - t_1)/4$; $C' = (T_C + t_1)/4$; $D' = (T_C - t_1)/4$; The other experimental parameters are as in a.

tween $^{13}C^\alpha$ and $^1H^\alpha$, which is active during t_1, the chemical shift of $^{13}C^\alpha$ is refocused. This leads to a superposition of multiplets corresponding to the two multiple quantum coherences $C^\alpha_{x,y}(i)C'_{x,y}(i-1)$ and $C^\alpha_{x,y}(i-1)C'_{x,y}(i-1)$, centered at the carbonyl frequency of the preceding residue and split by the one-bond $^{13}C^\alpha$-$^1H^\alpha$ scalar coupling. Of course, the assumption of uniform $^1J_{C\alpha H\alpha}$ scalar couplings might not be justified for all residues in a protein, as it was found that residues in extended β-sheet conformation display rather small values (140.5 ± 1.8 Hz), whereas larger magnitudes (146.5 ± 1.8 Hz) are found for α-helical residues (Vuister et al., 1992). In view of the small distribution within a given secondary structure element we do not expect significant variations of $^1J_{C\alpha H\alpha}$ for adjacent residues. In practice slight variations of $^1J_{C\alpha H\alpha}$ lead to a small shift of the peak maximum but should not affect the intensity ratio of the two multiplet components. The intensities of the two multiplet components are given by

$$I^a = I^a_i + I^a_{i-1} \tag{1a}$$

$$I^b = I^b_i + I^b_{i-1} \tag{1b}$$

where I^a and I^b are the downfield ($\omega_{C'} + \pi^1J_{C\alpha H\alpha}$) and upfield ($\omega_{C'} - \pi^1J_{C\alpha H\alpha}$) multiplet components of the two-spin coherences $C^\alpha_{x,y}(i)C'_{x,y}(i-1)$ (I^a_i and I^b_i) and $C^\alpha_{x,y}(i-1)C'_{x,y}(i-1)$ (I^a_{i-1} and I^b_{i-1}). The intensities of the individual multiplet components after the constant time delay T_C are given by

$$I^a_{i-1} = p_{i-1}\exp[+\Gamma^\Psi T_C] \tag{2a}$$

$$I^b_{i-1} = p_{i-1}\exp[-\Gamma^\Psi T_C] \tag{2b}$$

$$I^a_i = p_i\exp[+\Gamma^\varphi T_C] \tag{2c}$$

$$I^b_i = p_i\exp[-\Gamma^\varphi T_C] \tag{2d}$$

where p_i and p_{i-1} are the expectation values for intraresidue (N(i) to C^α(i)) and consecutive (N(i) to $C^\alpha(i-1)$) coherence transfer resulting from differences in the $^{1,2}J_{NC\alpha}$ scalar coupling constants. Additionally, the magnitudes of the expectation values are governed by the individual $^{13}C^\alpha$ autorelaxation rates R_{i-1} and R_i operative during the constant time delay T_C. Transverse relaxation of the $^{13}C'$ can be neglected, as it scales all individual multiplet components equally and thus does not influence the intensity ratio I^a/I^b. Γ^Ψ is the $^{13}C'(i-1)$ CSA-$^{13}C^\alpha$-$^1H^\alpha(i-1)$ dipolar cross-correlation rate (determined by the dihedral

angle Ψ), whereas Γ^{φ} is the $^{13}C'(i-1)$ CSA-$^{13}C^{\alpha}$-$^{1}H^{\alpha}(i)$ dipolar cross-correlation rate (determined by φ). Based on published $^{13}C^{\alpha}$ CSA values (Ye et al., 1993; Tjandra and Bax, 1997), we neglect $^{13}C'$-$^{1}H^{\alpha}$ dipolar and $^{13}C^{\alpha}$ CSA contributions, $\Gamma_{C\alpha,C'H\alpha}$ (Yang et al., 1998). For example, assuming $^{13}C^{\alpha}$ $\Delta\sigma = \sigma_{par} - \sigma_{ortho} = 40$ ppm, we estimate a value of 0.14 s^{-2} for $\Gamma_{C\alpha,C'H\alpha}/\tau_C$ [ns]. To discern the two cross-correlation rates (Γ^{Ψ} and Γ^{φ}), one has to know p_{i-1} and p_i, which are governed by the transfer amplitudes during the initial INEPT step and the decay rates of the transverse $^{13}C^{\alpha}$ magnetizations. To this end, a reference experiment (Figure 1b) was recorded with the same constant time delay and identical $^{13}C^{\alpha}$ inversion pulses, but refocusing $^{13}C^{\alpha}$-$^{1}H^{\alpha}$ scalar coupling evolution. The desired cross-correlation rate Γ^{φ} can be directly obtained from experimental intensity ratios I^a/I^b using Equations 2a–2d. The cross-correlation rate Γ^{Ψ} is known from a different experiment (Yang and Kay, 1998), and the expectation values p_{i-1} and p_i can be obtained from the reference experiment (Figure 1b). In the slow-motion limit, the cross-correlation rate Γ^{φ} is related to the dihedral angle by (Goldman, 1984):

$$\Gamma^{\varphi} = (4/15)(\mu_0/4\pi)(h/2\pi)\omega_C\gamma_C\gamma_H(r_{CH})^{-3} \times \tau_C(f_X + f_Y + f_Z) \quad (3)$$

where γ_i is the gyromagnetic ratio of nucleus i, $\omega_C = \gamma_C B_0$, r_{CH} is the $C^{\alpha}H^{\alpha}$ bond length, τ_C is the correlation time of the assumed rigid and isotropically tumbling molecule, and the factors f_i are projections of the dipolar vector onto the principal components of the carbonyl CSA tensor, $1/2(3\cos^2\theta_i - 1)$. The angles θ_i are related to the dihedral angle φ as follows:

$$\cos\theta_x = -0.3095 + 0.3531\cos(\varphi + 120°) \quad (4a)$$

$$\cos\theta_y = -0.1250 - 0.8740\cos(\varphi + 120°) \quad (4b)$$

$$\cos\theta_z = -0.9426\sin(\varphi + 120°) \quad (4c)$$

for non-glycine residues. For glycine residues, the cross correlation rate can be obtained from the intensity ratio of the most upfield and most downfield triplet component. Additionally, f_i has to be substituted by $f_{1i} + f_{2i}$, with $f_{1i} = f_i$ and f_{2i} is obtained by replacing $(\varphi + 120°)$ by $(\varphi - 120°)$. Note that the $^{13}C'$ selective 90° pulses are applied as hard pulses employing rf field strengths adjusted to $\Delta/\sqrt{15}$, where Δ is the difference between $^{13}C^{\alpha}$ and $^{13}C'$ chemical shift regions, which leads to a slight decrease in peak intensities for glycines. Ser and Leu residues typically exhibit only small shift differences between $^{13}C^{\alpha}$ and $^{13}C^{\beta}$. In this case, the shaped 180° pulse in the middle of the constant time relaxation delay does not selectively invert the $^{13}C^{\alpha}$ spins, thus giving rise to signal modulation due to the one-bond $^{13}C^{\alpha}$-$^{13}C^{\beta}$ coupling. The $^{1}J_{C\alpha C\beta}$ coupling constant is active during the entire constant time delay T_C and the signal intensity is modulated by $\cos(\pi^{1}J_{C\alpha C\beta}T_C)$. Using T_C values of 26 ms, this leads to a sign change of the signals for serines and leucines in the reference experiment. Accordingly, the resulting multiplet intensity is governed by the difference of the two contributions ($[I^{i-1} - I^{i}]$ for Ser, Thr and Leu; $[-I^{i-1} + I^{i}]$ for residues following Ser, Thr and Leu in the sequence).

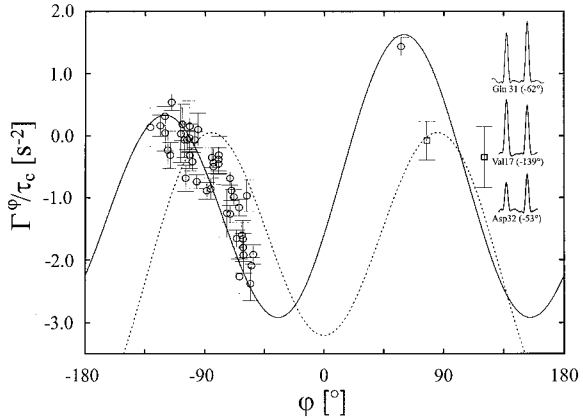

Figure 2. Correlation between calculated and experimental values of Γ^{φ} ($\Gamma_{H^{\alpha}C^{\alpha}}(i),C'(i-1)$) for non-glycine (solid line; open circles) and glycine (dotted line; open squares) residues in ubiquitin (Wand et al., 1996). Values of 244, 178 and 90 ppm were used for σ_{xx}, σ_{yy} and σ_{zz} (Teng et al., 1992). Representative F_1 cross sections are illustrated. A 1.5 mM ubiquitin sample, 50 mM phosphate buffer, pH = 5.5, 26 °C was employed and a total measuring time of 24 h was used to record the 3D data set using the pulse sequence of Figure 1a [T_C = 26 ms, 25×25×512 complex points with acquisition times of 20.8, 15.1 and 64 ms in (t_1,t_2,t_3)]. The reference experiment (Figure 1b) was recorded with identical parameters. All spectra were recorded on a Varian Unity+ 500 MHz spectrometer, data were processed and analyzed using the programs NMRPipe (Delaglio et al., 1995) and PIPP/CAPP (Garrett et al., 1991).

Figure 2 shows the Γ^{φ} versus φ profile obtained on ^{13}C,^{15}N-labeled ubiquitin (Wand et al., 1996). Cross sections through respective 2D planes for residues Val17, Gln31 and Asp32 are also shown in Figure 2. To assess the experimental applicability of the newly devised sequence, we calculated the S/N ratio of the relaxation experiment (Figure 1a) and the reference experiment (Figure 1b) and compared it to the already existing sequence for the determination of the dihedral angle Ψ (Yang et al., 1998) (Table 1). Additionally, we

Table 1. Signal-to-noise ratio of the three experiments used for the derivation of the cross-correlation rate Γ^{φ}

Experiment	S/N
Γ^{Ψ} (Yang and Kay, 1998)	$69 \pm 25 / 67 \pm 24$[a]
Γ^{φ} (Figure 1a)	$49 \pm 15 / 45 \pm 12$[a]
Reference (Figure 1b)	$52 \pm 21 / 22 \pm 5$[b]

[a] For Γ^{Ψ} and Γ^{φ} two S/N values corresponding to the two multiplet components are given.

[b] The two S/N values denote the intra-residue and consecutive cross peak intensities, respectively.

did a careful analysis of the error propagation based on Monte Carlo error analysis (Palmer et al., 1991). The precision limit of the obtained cross-correlation rate Γ^{φ} was derived from Monte Carlo simulations of the distributions of the experimental differential peak intensities and optimized cross-correlation rates. The root-mean-square baseline noises in the three experiments were taken as a measure of the standard deviations of the peak heights in these experiments. 100 000 simulated data sets were chosen at random from these distributions and the cross-correlation rate Γ^{φ} was extracted from Equations 2a–2d. The average error was calculated to be 0.40 ± 0.06 s^{-1} for glycine residues, 0.14 ± 0.03 s^{-1} for residues adjacent to glycines and 0.24 ± 0.09 s^{-1} for other residues.

On average, the agreement between experimental Γ^{φ} rates and theoretical values calculated from φ values of the X-ray structure (Vijay-Kumar et al., 1987) is comparable to analogous pulse schemes (Yang et al., 1997, 1998) for the backbone dihedral angle Ψ. Some deviations occur, which we believe are due to the presence of internal backbone dynamics at these molecular sites. For example, anisotropic local motion of an individual peptide plane (Bremi and Brüschweiler, 1997) would scale the three orthogonal C′ CSA tensor components differently and can induce significant changes in the $^{13}C'/^{13}C^{\alpha}$-$^{1}H^{\alpha}$ CSA-dipolar cross-correlation rates.

In summary, a pulse sequence has been presented for measuring $^{13}C'(i-1)$ $^{13}C^{\alpha}(i)$-$^{1}H^{\alpha}(i)$ CSA dipole cross-correlation rates in uniformly ^{13}C,^{15}N-enriched proteins. It complements information from $^{13}C^{\alpha}(i)$-$^{1}H^{\alpha}(i)$ dipolar/$^{15}N(i)$-$^{1}H^{N}(i)$ dipolar cross-correlated spin relaxation rates and can be used to unambiguously determine the backbone dihedral angle φ in proteins. Additionally, the experiment will be instrumental to monitor locally anisotropic internal backbone dynamics in proteins.

Acknowledgements

The authors thank Prof. A.J. Wand (University of Pennsylvania) for kindly supplying uniformly ^{13}C,^{15}N-labeled ubiquitin. This research was supported by grant P 13486 from the Austrian Science Foundation FWF.

References

Bremi, T. and Brüschweiler, R. (1997) *J. Am. Chem. Soc.*, **119**, 6672–6673.
Chiarparin, E., Pelupessy, P., Ghose, R. and Bodenhausen, G. (1999) *J. Am. Chem. Soc.*, **121**, 6876–6883.
Delaglio, F., Grzesiek, S., Vuister, G.W., Zhu, G., Pfeifer, J. and Bax, A. (1995) *J. Biomol. NMR*, **6**, 277–293.
Garrett, D.S., Powers, P., Gronenborn, A.M. and Clore, G.M. (1991) *J. Magn. Reson.*, **95**, 214–220.
Geen, H. and Freeman, R. (1991) *J. Magn. Reson.*, **93**, 93–141.
Goldman, M. (1984) *J. Magn. Reson.*, **60**, 437–452.
Kay, L.E., Keifer, P. and Saarinen, T. (1992) *J. Am. Chem. Soc.*, **114**, 10663–10665.
Kupce, E., Boyd, J. and Campbell, I.D. (1995) *J. Magn. Reson.*, **B106**, 300–303.
Kupce, E. and Freeman, R. (1995) *J. Magn. Reson.*, **A115**, 273–276.
Marion, D., Ikura, M., Tschudin, R. and Bax, A. (1989) *J. Magn. Reson.*, **85**, 393–399.
Palmer III, A.G., Rance, M. and Wright, P.E. (1991) *J. Am. Chem. Soc.*, **113**, 4371–4380.
Pelupessy, P., Chiarparin, E., Ghose, R. and Bodenhausen, G. (1999) *J. Biomol. NMR*, **14**, 277–280.
Reif, B., Hennig, M. and Griesinger, C. (1997) *Science*, **276**, 1230–1233.
Schleucher, J., Sattler, M. and Griesinger, C. (1993) *Angew. Chem. Int. Ed. Engl.*, **32**, 1489–1491.
Shaka, A.J., Keeler, J., Frenkiel, T. and Freeman, R. (1983) *J. Magn. Reson.*, **52**, 335–338.
Teng, Q., Iqbal, M. and Cross, T.A. (1992) *J. Am. Chem. Soc.*, **114**, 5312–5321.
Tjandra, N. and Bax, A. (1997) *J. Am. Chem. Soc.*, **119**, 9576–9577.
Vijay-Kumar, S., Bugg, C.E. and Cook, W.J. (1987) *J. Mol. Biol.*, **194**, 531–544.
Vuister, G.W. and Bax, A. (1992) *J. Magn. Reson.*, **98**, 428–435.
Vuister, G.W., Delaglio, F. and Bax, A. (1992) *J. Am. Chem. Soc.*, **114**, 9674–9675.
Wand, A.J., Urbauer, J.L., McEvoy, R.P. and Bieber, R.J. (1996) *Biochemistry*, **35**, 6116–6125.
Yang, D., Konrat, R. and Kay, L.E. (1997) *J. Am. Chem. Soc.*, **119**, 11938–11940.
Yang, D., Gardner, K.H. and Kay, L.E. (1998) *J. Biomol. NMR*, **11**, 1–8.
Yang, D. and Kay, L.E. (1998) *J. Am. Chem. Soc.*, **120**, 9880–9887.
Ye, C., Fu, R., Hu, J., Hou, L. and Ding, S. (1993) *Magn. Reson. Chem.*, **31**, 699–704.